



Published in final edited form as:

Nat Cell Biol. ; 14(4): 409–415. doi:10.1038/ncb2447.

Cdk5 and Mekk1 mediate a Pro-Apoptotic Signaling Response to Endoplasmic Reticulum Stress in a *Drosophila* Model of Autosomal Dominant Retinitis Pigmentosa

Min-Ji Kang, Jaehoon Chung, and Hyung Don Ryoo

Department of Cell Biology, New York University School of Medicine 550 First Avenue, New York, NY 10016

Abstract

Chronic stress in the endoplasmic reticulum (ER) underlies many degenerative and metabolic diseases involving apoptosis of vital cells. A well-established example is Autosomal Dominant Retinitis Pigmentosa (ADRP), an age-related retinal degenerative disease caused by mutant rhodopsins^{1,2}. Similar mutant alleles of *Drosophila* rhodopsin-1 also impose stress on the ER and cause age-related retinal degeneration in that organism³. Well-characterized signaling responses to ER-stress, referred to as the Unfolded Protein Response (UPR)⁴, induce various ER quality control genes that can suppress such retinal degeneration⁵. However, how cells activate cell death programs after chronic ER-stress remains poorly understood. Here, we report the identification of a signaling pathway mediated by *cdk5* and *mekk1* required for ER-stress-induced apoptosis. Inactivation of these genes specifically suppressed apoptosis, without affecting other protective branches of the UPR. Cdk5 phosphorylates Mekk1, and together, activate the JNK pathway for apoptosis. Moreover, disruption of this pathway can delay the course of age-related retinal degeneration in a *Drosophila* model of ADRP. These findings establish a previously unrecognized branch of ER-stress response signaling involved in degenerative diseases.

Three branches of the Unfolded Protein Response (UPR) are particularly well characterized in mammals and conserved in *Drosophila*⁴. In brief, these pathways involve transmembrane proteins ATF6, IRE1 and PERK, respectively, that can sense stress in the ER lumen. ATF6 is a transcription factor anchored to the ER membrane that translocates to the nucleus after ER-stress triggers its proteolysis, and IRE1 is an endonuclease that activates the transcription factor XBP1 through an unconventional mRNA splicing mechanism. PERK is an ER-stress responsive kinase that mediates the translational activation of the transcription factor, ATF4. The predominant effect of these pathways is to reduce stress in the ER and help the cells return to their normal physiological state. Consistently, the major targets of these transcription factors include genes that encode ER chaperones, anti-oxidant proteins and those involved in misfolded protein degradation^{6–8}.

Users may view, print, copy, download and text and data- mine the content in such documents, for the purposes of academic research, subject always to the full Conditions of use: http://www.nature.com/authors/editorial_policies/license.html#terms

Corresponding Author: Hyung Don Ryoo Tel: 212-263-7257 Hyungdon.Ryoo@nyumc.org.

Author Contributions M. K and H.D.R. designed the experiments. J.C. carried out the EP screen. All other experiments were performed by M. K. H.D.R. wrote the paper and all authors read and edited the manuscript.

Our in vivo model for ER-stress-induced apoptosis is based on a mutant *Drosophila* Rhodopsin-1 (Rh-1) allele, Rh-1^{G69D}, which is similar in nature with human rhodopsin mutants that underlie retinal degeneration in Autosomal Dominant Retinitis Pigmentosa (ADRP)^{9, 10}. While the endogenous allele causes late-onset retinal degeneration without affecting the external eye morphology, overexpression of this encoded protein in larval eye imaginal discs (during photoreceptor differentiation) led to an easily identifiable adult eye phenotype by eclosion (Figure 1A, B, Supplementary Figure S1B). The adult eye was abnormally small, indicative of massive cell loss, and the surviving eye tissue showed a glassy surface that was devoid of ommatidial structures. The effect of Rh-1^{G69D} overexpression can be attributed to excessive ER-stress for the following reasons: The Rh-1^{G69D} overexpression phenotype was suppressed by the co-expression of *Drosophila hrd1* (Supplementary Figure S1C), which encodes an E3 ubiquitin ligase dedicated to degrading misfolded ER proteins⁵. In addition, we detected signs of ER stress using two independent reporters. One is the XBP1-EGFP reporter, which expresses EGFP in frame only when ER-stress stimulates IRE1-dependent XBP1 mRNA splicing³. This reporter was activated in Rh-1^{G69D} misexpressing imaginal discs while not active in control tissues (Supplementary Figure S1D, E). We were also able to detect signs of ER-stress through an antibody against *Drosophila* ATF4. This protein is encoded in the *cryptocephal* (*crc*) locus¹¹. As in mammals¹², we found that the *Drosophila* ATF4 expression was induced after ER stress (Supplementary Figure S1F, G, H). Expression of Rh-1^{G69D} in eye imaginal discs also increased the level of endogenous superoxides as evidenced by Dihydroethidium (DHE) labeling (Supplementary Figure S1J, K), consistent with previous reports of elevated ROS in stressed ER¹³⁻¹⁷. Co-expressing Hrd1 suppressed such induction of ATF4 and ROS (Supplementary Figure S1I, L), indicating that these markers appear as a result of misfolded protein overload in the ER.

An easily detectable adult eye phenotype allowed us to conduct an in vivo RNAi screen to identify genes required for Rh-1^{G69D}-induced toxicity. We specifically focused on kinases and phosphatases that could serve as signaling proteins potentially linking the distressed ER and the apoptotic machinery. Of the 196 protein kinases and 66 protein phosphatases encoded in the *Drosophila* genome¹⁸, we were able to target 119 kinases and 39 phosphatases through RNAi mediated knock down, using a total of 276 inverted repeat transgenes available from the Vienna *Drosophila* RNAi Center (Supplementary Information, Table 1). We found three lines that strongly suppressed the adult eye phenotype, two of which (VDR35855 and VDR35856) targeted *Drosophila cdk5* (Figure 1C). Cdk5 is an atypical cyclin-dependent kinase with established roles in differentiated postmitotic cells, such as neurons, adipose tissue and pancreatic beta-islet cells¹⁹⁻²². In mammals, Cdk5 is reportedly activated by various stress conditions, including those that disrupt ER function²³. Excessive activation of Cdk5 contributes to neurotoxicity in Alzheimer's and Parkinson's Diseases models^{24, 25}. We found that *cdk5* knockdown did not affect an independent cell death phenotype caused by p53-overexpression in the eye (Figure 1E, F). These results indicate that *cdk5* mediates a specific signaling response to mutant Rh-1, rather than affecting the general cell death machinery. When eye imaginal discs were inspected, we noticed a dramatic reduction of TUNEL positive cells, indicating that *cdk5* is required for apoptosis in this assay (Figure 1G, H). To test whether Cdk5 has a conserved role in

mammals, we used mouse Min6 cells, which readily succumb to apoptosis when treated with tunicamycin (Supplementary Figure S2), a compound that inhibits protein glycosylation and cause stress in the ER²⁶. Knockdown of Cdk5 strongly suppressed tunicamycin-induced apoptosis, as assessed through TUNEL labeling (Supplementary Figure S2). Cdk5 levels did not change in response to Rh-1^{G69D} expression (Figure 1U, V), suggesting that the protein is regulated by post-transcriptional mechanisms. In fact, Cdk5 activity is often regulated through its regulatory subunit, p35 (also known as Cdk5alpha)²⁷. In a loss of function *p35* (*Cdk5alpha*) background, the amount of apoptosis induced by Rh-1^{G69D} expression was significantly reduced (Figure 1I, J), further confirming the role of Cdk5 in apoptosis.

To determine if the *cdk5* knockdown condition suppresses apoptosis by reducing the overall stress levels in the ER, we labeled imaginal discs with the anti-ATF4 antibody. The degree of ATF4 induction in Rh-1^{G69D} overexpressing eye discs was not affected by *cdk5* knockdown (Figure 1K–M). We also assessed the extent of IRE1/XBP1 pathway activation, using the XBP1-EGFP reporter. Again, knockdown of *cdk5* did not affect the degree of this ER stress reporter activation in response to Rh-1^{G69D} expression (Figure 1N–P). These observations indicate that *cdk5* mediates Rh-1^{G69D}-induced apoptosis without affecting the overall levels of misfolded protein load in the ER. To further test if the ATF4 and IRE1/XBP1 pathways contribute to Rh-1^{G69D}-induced apoptosis, we examined the degree of cell death in mutants that disrupt these pathways. In the loss of function ATF4 condition, *crc* ^{-/-}₃₂, the degree of Rh-1^{G69D}-induced apoptosis was similar to those of the *crc*⁺ background (Figure 1Q, R). In the *ire1* ^{-/-} mosaic clones, the degree of Rh-1^{G69D}-induced apoptosis was increased (Figure 1S, T). Overall, these results show that ATF4 and IRE1 are not required for Rh-1^{G69D} expression to induce apoptosis.

Independently, we performed a gene overexpression screen with Epgy2 lines²⁸ for modifiers of the *gmr-Gal4* driven Rh-1 overexpression phenotype (Supplementary Figure S3). While a wild type Rh-1 transgene was used in this experimental setup, the system drives the expression of Rh-1 beyond the folding capacity of the imaginal disc cells, as indicated by the activation of ER stress reporters⁵. We specifically screened 400 lines with insertions in the 3rd chromosomes that were associated with genes with annotated function and scored a total of six suppressors. Among these suppressors were expected ones, including a line associated with *hrd1* (*P{EPgy2}sip3[EY11980]*), whose effect on the Rh-1^{G69D} misexpression phenotype was independently validated in Supplementary Figure S1. Another expected suppressor line was *P{EPgy2}th[EY00710]*, with *P{EPgy2}* element inserted upstream of the anti-apoptotic gene, *Drosophila* IAP1 (Diap1)²⁹, indicating that excessive apoptosis contributes to the Rh-1 overexpression phenotype.

We also identified an enhancer of the Rh-1 overexpression phenotype, *EY02276*, associated with the *mekk1* locus. Previous studies have characterized *mekk1* as an osmotic stress response gene that lies upstream of JNK and p38 kinases^{30, 31}. This line did not show any overexpression associated phenotype on its own, but enhanced the Rh-1 overexpression phenotype when co-expressed (Supplementary Figure S3). Conversely, the Rh-1^{G69D} misexpression phenotype was suppressed in the *mekk1^{ur-36}* ^{-/-} background (Figure 2A–C). Upon inspection of imaginal discs, we found that the *mekk1^{ur-36}* ^{-/-} background almost

completely suppressed apoptosis triggered by Rh-1^{G69D}-overexpression (Figure 2D–F). To determine if *mekk1* affects the overall levels of stress in the ER, we assessed the degree of XBP1-EGFP and ATF4 activation in eye imaginal discs overexpressing Rh-1^{G69D}. We found no discernible difference between the *mekk1*⁺ and *mekk1*^{UR-36} ^{–/–} discs in the level of these ER stress reporters (Figure 2G–L), indicating that *mekk1* specifically mediates the pro-apoptotic signaling response without affecting the degree of ER-stress. To further test the role of *mekk1* in ER-stress-induced toxicity, we subjected *mekk1* ^{–/–} adults to an independent assay, in which the flies were fed tunicamycin and their survival rate was monitored. While control wild type flies were vulnerable to this regimen, with only 15.7% of the flies surviving after 7 days of tunicamycin feeding, the survival rate of *mekk1* ^{–/–} flies was much higher under identical conditions (57.8%). Three independent trials of this assay gave a statistically significant difference in the survival rate of *mekk1* mutant flies ($p=0.0062$) (Figure 2M).

As previous studies have placed *mekk1* genetically upstream of JNK³⁰, we examined the relationship between JNK, Mekk1 and Cdk5. For this, we exposed *Drosophila* S2 cells to thapsigargin (Tg), a SERCA inhibitor that is widely used to cause ER stress in cells³². Phospho-JNK appeared after 2 hours of Tg treatment (Figure 3A), and this induction of JNK phosphorylation was suppressed upon knockdown of *cdk5* or *mekk1* (Figure 3A), or when cells were treated with the Cdk5 inhibitor, roscovitine (Figure 3B). On the other hand, knockdown of other known mediators of the UPR, such as *ire1*, *traf4*, *perk* and *atf6* had no discernible effects on JNK phosphorylation (Figure 3A). Among other stress conditions tested, H₂O₂ treatment generated a similar outcome (Figure 3C–F). H₂O₂'s ability to induce JNK phosphorylation was significantly reduced in S2 cells pretreated with dsRNA targeting *cdk5* or *mekk1*. While H₂O₂ treatment resulted in a more than six fold increase in phospho-JNK levels in control cells, *cdk5* knocked down cells had on average only a two fold increase in phospho-JNK induction (Figure 3D)($n=3$, $p=0.018$). Likewise, *mekk1* knockdown reduced the extent of phospho-JNK induction in a statistically significant manner (Figure 3F)($n=3$, $p=0.0023$).

Consistent with the results from S2 cells, Rh-1^{G69D} misexpressing imaginal discs showed signs of JNK signaling activation, as assessed through the *puc-lacZ* reporter (Figure 3G–I). To test if JNK is required for ER-stress-induced apoptosis, we generated loss-of-function mosaic clones of the *Drosophila* JNK gene, *basket*. When Rh-1^{G69D} was overexpressed in imaginal discs harboring *basket* ^{–/–} clones, the number of apoptotic cells as assessed through TUNEL labeling was significantly reduced, with the remaining apoptotic cells primarily within the *basket*⁺ mosaic clones (Figure 3J–L). We noticed that many apoptotic cells were found at the clonal boundaries. This property was also observed in mutant mosaic clones of *dronc* (Supplementary Figure S4), which is an essential initiator caspase for apoptosis³³³⁴. These observations support the idea that ER-stress activates Cdk5/Mekk1-mediated JNK signaling to cause caspase-dependent apoptosis.

Using a phosphorylation site prediction program (<http://scansite.mit.edu>), we detected two consensus Cdk5 phosphorylation sites within the *Drosophila melanogaster* Mekk1 protein sequence, T157 and S1127. The putative phosphorylation sites within Mekk1 were conserved in other *Drosophila* species, suggestive of its functional significance (Figure 4A).

To test if Mekk1 is in fact phosphorylated by Cdk5, we generated antibodies directed against the putative phospho-residues (see Methods). Using one of these, an antibody directed towards the phosphorylated S1127 residue, we were able to detect Mekk1 phosphorylation by Cdk5 in vitro (Figure 4B). We also detected phosphorylation of this residue in cultured HEK293T cells transfected with flag-tagged Mekk1 (Figure 4C). Notably, the intensity of the phospho-S1127 band increased significantly in cells when Cdk5 was co-transfected, and further enhanced when those cells were stressed with H₂O₂ (Figure 4C lanes 3, 4). On average, the degree of Mekk1 phosphorylation increased more than three fold after H₂O₂ treatment (Figure 4C, $n=3$, $p=0.0003$). We confirmed that this band corresponds to phospho-S1127, as the signal did not appear when the Mekk1 S1127 residue was mutated (Figure 4D lane 5, 6). Furthermore, the anti-phospho-Mekk1 failed to detect any band when the immunoprecipitate was treated with the lambda phosphatase (Figure 4E). Moreover, the two proteins physically interacted, as evidenced by co-immunoprecipitation assays. Interestingly, the interaction was enhanced when the cells were pre-treated with H₂O₂ (Figure 4F). Taken together, these genetic and biochemical experiments support the idea that Cdk5 and Mekk1 form a pathway to activate JNK signaling in response to ER-stress.

To test if this pro-apoptotic signaling pathway is also relevant to an age-dependent disease process, we turned to the *Drosophila* model for ADRP, where an endogenous mutant allele of the Rh-1 gene, *ninaE*^{G69D}, causes late-onset retinal degeneration phenotype associated with ER stress^{9, 10}. To track the course of retinal degeneration in live flies, we used the *ninaE*^{G69D/+} condition combined with a Rh-1>GFP reporter³⁵. Nearly 90% of *ninaE*^{G69D/+} flies lost the regular ommatidial array by day 28 after eclosion, indicative of age-related retinal degeneration. Those *ninaE*^{G69D/+} flies in a *mekk1*^{ur-36} -/- background showed a delayed course of retinal degeneration, with only about half of the examined flies with disrupted Rh-1>GFP patterns (Figure 5A). Knockdown of *cdk5* in the photoreceptors also delayed the course of retinal degeneration to a similar degree (Figure 5F). This result was further validated through tangential sections of 20 day old fly retina. Wild type flies showed regular ommatidial arrays (Figure 5B), while the *ninaE*^{G69D/+} retina by this age showed disorganized ommatidia (Figure 5C, G). This phenotype was largely rescued in the backgrounds of *mekk1*^{ur-36} -/- (Figure 5D), or in *cdk5* knockdown conditions (Figure 5H).

These results indicate that the pro-apoptotic ER-stress response mediated by *mekk1* and *cdk5* are relevant to understanding age-related photoreceptor degeneration in ADRP. Moreover, our results suggest that Cdk5/Mekk1/JNK forms a pathway that is independent of those UPR branches. While it is unclear what lies upstream of Cdk5 in our experimental system, we note that among the previously characterized Cdk5 activating signals include ROS, calpains and Cam kinase II^{23, 25, 36, 37}, which have been also associated with ER-stress^{16, 38}. Thus it is possible to envision a model where chronic proteotoxicity in the ER sends Cdk5 activating signals to the cytoplasm, perhaps via ROS or Ca²⁺ mediated signaling. Once Cdk5 is activated, it may send pro-apoptotic signals to the nucleus through the Mekk1/JNK pathway (Supplementary Figure S5).

Many terminally differentiated cells without regenerative potential are known to acquire resistance to apoptosis during differentiation. In *Drosophila*, such apoptotic resistance can be attributed to the epigenetic silencing of major pro-apoptotic gene loci during

development³⁹. A recent study showed that one of the consequences of stress-induced Mekk1-signaling is to induce the expression of genes that are normally silenced through epigenetic mechanisms³¹. Based on these observations, we think it is possible that terminally differentiated photoreceptors may have their pro-apoptotic loci in heterochromatin-like states, and stress-induced Cdk5/Mekk1 pathway contributes to neurodegeneration by restoring those loci to an open chromatin state, an idea that needs to be tested through future studies.

Supplementary Material

Refer to Web version on PubMed Central for supplementary material.

Acknowledgements

We thank Ed Giniger, Kunihiko Matsumoto, Masayuki Miura, the VDRC and Bloomington stock centers for reagents, Edith Robbins, Michele Pagano and Ester Zito for technical advice, and David Ron for discussions and critical comments on the manuscript. This work was supported by the National Institutes of Health grant R01EY020866. H.D.R. is an Ellison Medical Foundation New Scholar.

Reference

1. Dryja T, McGee TL, Reichel E, Hahn LB, Cowley GS, Yandell DW, Sandberg MA, Berson EL. A point mutation of the rhodopsin gene in one form of retinitis pigmentosa. *Nature*. 1990; 343:364–366. [PubMed: 2137202]
2. Sung CH, Davenport CM, Hennessey JC, Maumenee IH, Jacobson SG, Heckenlively JR, Nowakowski R, Fishman G, Gouras P, Nathans J. Rhodopsin mutations in autosomal dominant retinitis pigmentosa. *Proc. Natl. Acad. Sci. U.S.A.* 1991; 88:6481–6485. [PubMed: 1862076]
3. Ryoo HD, Domingos PM, Kang MJ, Steller H. Unfolded protein response in a *Drosophila* model for retinal degeneration. *Embo J.* 2007; 26:242–252. [PubMed: 17170705]
4. Walter P, Ron D. The unfolded protein response: from stress pathway to homeostatic regulation. *Science*. 2011; 334:1081–1086. [PubMed: 22116877]
5. Kang M-J, Ryoo HD. Suppression of retinal degeneration in *Drosophila* by stimulation of ER-Associated Degradation. *Proc. Natl. Acad. Sci. U.S.A.* 2009; 106:17043–17048. [PubMed: 19805114]
6. Travers KJ, Patil CK, Wodicka L, Lockhart DJ, Weissman JS, Walter P. Functional and genomic analyses reveal an essential coordination between the unfolded protein response and ER-associated degradation. *Cell*. 2000; 101:249–258. [PubMed: 10847680]
7. Harding HP, et al. An integrated stress response regulates amino acid metabolism and resistance to oxidative stress. *Mol Cell*. 2003; 11:619–633. [PubMed: 12667446]
8. Yamamoto K, Sato T, Matsui T, Sato M, Okada T, Yoshida H, Harada A, Mori K. Transcriptional induction of mammalian ER quality control proteins is mediated by single, or combined action of ATF6alpha and xbp1. *Dev. Cell*. 2007; 13:365–376. [PubMed: 17765680]
9. Colley NJ, Cassill JA, Baker EK, Zuker CS. Defective intracellular transport is the molecular basis of rhodopsin-dependent dominant retinal degeneration. *Proc. Natl. Acad. Sci. U.S.A.* 1995; 92:3070–3074. [PubMed: 7708777]
10. Kurada P, O'Tousa JE. Retinal degeneration caused by dominant rhodopsin mutations in *Drosophila*. *Neuron*. 1995; 14:571–579. [PubMed: 7695903]
11. Hewes RS, Schaefer AM, Taghert PH. The *cryptocephal* gene (*ATF4*) encodes multiple basic-leucine zipper proteins controlling molting and metamorphosis in *Drosophila*. *Genetics*. 2000; 155:1711–1723. [PubMed: 10924469]
12. Harding HP, Novoa I, Zhang Y, Zeng H, Wek R, Schapira M, Ron D. Regulated translation initiation controls stress-induced gene expression in mammalian cells. *Mol. Cell*. 2000; 6:1099–1108. [PubMed: 11106749]

13. Marciniak SJ, et al. CHOP induces death by promoting protein synthesis and oxidation in the stressed endoplasmic reticulum. *Genes Dev.* 2004; 18:3066–3077. [PubMed: 15601821]
14. Li G, Scull C, Ozcan L, Tabas I. NADPH oxidase links endoplasmic reticulum stress, oxidative stress and PKR activation to induce apoptosis. *J. Cell Biol.* 2010; 191:1113–1125. [PubMed: 21135141]
15. Song B, Scheuner D, Ron D, Pennathur S, Kaufman RJ. Chop deletion reduces oxidative stress, improves beta cell function, and promotes cell survival in multiple mouse models of diabetes. *J. Clin. Invest.* 2008; 118:3378–3389. [PubMed: 18776938]
16. Timmins JM, Ozcan L, Seimon TA, Malagelada C, Backs J, Backs T, Bassel-Duby R, Olson EN, Anderson ME, Tabas I. Calcium/calmodulin-dependent protein kinase II links ER stress with Fas and mitochondrial apoptosis pathways. *J. Clin. Invest.* 2009; 119:2925–2941. [PubMed: 19741297]
17. Tu BP, Weissman JS. Oxidative protein folding in eukaryotes: mechanisms and consequences. *J. Cell Biol.* 2004; 164:341–346. [PubMed: 14757749]
18. Morrison DK, Murakami MS, Cleghon V. Protein kinases and phosphatases in the *Drosophila* genome. *J. Cell Biol.* 2000; 150:57–62.
19. Connell-Crowley L, Le Gall M, Giniger E. The cyclin-dependent kinase cdk5 controls multiple aspects of axon patterning in vivo. *Curr. Biol.* 2000; 10:599–602. [PubMed: 10837225]
20. Tsai LH, Delalle I, Caviness VS, Chae T, Harlow E. p35 is a neural-specific regulatory subunit of cyclin-dependent kinase 5. *Nature.* 1994; 371:419–423. [PubMed: 8090221]
21. Choi JH, Banks AS, Estall JL, Kajimura S, Bostrom P, Laznik D, Ruas JL, Chalmers MJ, Kamenecka TM, Bluher M, Griffin PR, Spiegelman BM. Anti-diabetic drugs inhibit obesity-linked phosphorylation of PPARgamma by Cdk5. *Nature.* 2010; 466:451–456. [PubMed: 20651683]
22. Wei FY, Nagashima K, Ohshima T, Saheki Y, Lu YF, Matsushita M, Yamada Y, Mikoshiba K, Seino Y, Matsui H, Tomizawa K. Cdk5-dependent regulation of glucose-stimulated insulin secretion. *Nat. Med.* 2005; 11:1104–1108. [PubMed: 16155576]
23. Saito T, Konno T, Hosokawa T, Asada A, Ishiguro K, Hisanaga S. p25/cyclin-dependent kinase 5 promotes the progression of cell death in nucleus of endoplasmic reticulum-stressed neurons. *J. Neurochem.* 2007; 102:133–140. [PubMed: 17506859]
24. Patrick GN, Zukerberg L, Nikolic M, de la Monte S, Dikkes P, Tsai LH. Conversion of p35 to p25 deregulates Cdk5 activity and promotes neurodegeneration. *Nature.* 1999; 402:615–622. [PubMed: 10604467]
25. Qu D, Rashidian J, Mount MP, Aleyasin H, Persanejad M, Lira A, Haque E, Zhang Y, Callaghan S, Daigle M, Rousseaux MW, Slack RS, Albert PR, Vincent I, Woulfe JM, Park DS. Role of Cdk5-mediated phosphorylation of Prx2 in MPTP toxicity and Parkinson's disease. *Neuron.* 2007; 55:37–52. [PubMed: 17610816]
26. Elbein AD. Inhibitors of glycoprotein synthesis. *Methods Enzymol.* 1983; 98:135–154. [PubMed: 6669046]
27. Connell-Crowley L, Vo D, Luke L, Giniger E. *Drosophila* lacking the Cdk5 activator, p35, display defective axon guidance, age-dependent behavioral deficits and reduced lifespan. *Mech. Dev.* 2007; 124:341–349. [PubMed: 17368005]
28. Rorth P. A modular misexpression screen in *Drosophila* detecting tissue-specific phenotypes. *Proc. Natl. Acad. Sci. U.S.A.* 1996; 93:12418–12422. [PubMed: 8901596]
29. Hay BA, Wasserman DA, Rubin GM. *Drosophila* homologs of baculovirus inhibitor of apoptosis proteins function to block cell death. *Cell.* 1995; 83:1253–1262. [PubMed: 8548811]
30. Inoue H, Tateno M, Fujimura-Kamada K, Takaesu G, Adachi-Yamada T, Ninomiya-Tsuji J, Irie K, Nishida Y, Matsumoto K. A *Drosophila* MAPKKK, D-Mekk1, mediates stress response through activation of p38 MAPK. *EMBO J.* 2001; 20:5421–5430. [PubMed: 11574474]
31. Seong KH, Li D, Shimizu H, Nakamura R, Ishii S. Inheritance of stress-induced, ATF-2-dependent epigenetic change. *Cell.* 2011; 145:1049–1061. [PubMed: 21703449]
32. Lytton J, Westlin M, Hanley MR. Thapsigargin inhibits the sarcoplasmic or endoplasmic reticulum Ca-ATPase family of calcium pumps. *J. Biol. Chem.* 1991; 266:17067–17071. [PubMed: 1832668]

33. Chew SK, Akdemir F, Chen P, Lu WJ, Mills K, Daish T, Kumar S, Rodriguez A, Abrams JM. The apical caspase Dronc governs programmed and unprogrammed cell death in *Drosophila*. *Dev. Cell.* 2004; 7:897–907. [PubMed: 15572131]
34. Xu D, Li Y, Arcaro M, Lackey M, Bergmann A. The CARD-carrying caspase Dronc is essential for most, but not all, developmental cell death in *Drosophila*. *Development.* 2005; 132:2125–2134. [PubMed: 15800001]
35. Pichaud F, Desplan C. A new visualization approach for identifying mutations that affect differentiation and organization of the *Drosophila* ommatidia. *Development.* 2001; 128:815–826. [PubMed: 11222137]
36. Lee MS, Kwon YT, Li M, Peng J, Friedlander RM, Tsai LH. Neurotoxicity induces cleavage of p35 to p25 by calpain. *Nature.* 2000; 405:360–364. [PubMed: 10830966]
37. Dhavan R, Greer PL, Morabit MA, Orlando LR, Tsai LH. The cyclin-dependent kinase 5 activators p35 and p39 interact with the alpha-subunit of Ca²⁺/calmodulin-dependent protein kinase II and alpha-actinin-1 in a calcium-dependent manner. *J. Neurosci.* 2002; 22:7879–7891. [PubMed: 12223541]
38. Nakagawa T, Yuan J. Cross-talk between two cysteine protease families. Activation of caspase-12 by calpain in apoptosis. *J Cell Biol.* 2000; 150:887–894. [PubMed: 10953012]
39. Zhang Y, Lin N, Carroll PM, Chan G, Guan B, Xiao H, Yao B, Wu SS, Zhou L. Epigenetic blocking of an enhancer region controls irradiation-induced proapoptotic gene expression in *Drosophila* embryos. *Dev. Cell.* 2008; 14:481–493. [PubMed: 18410726]

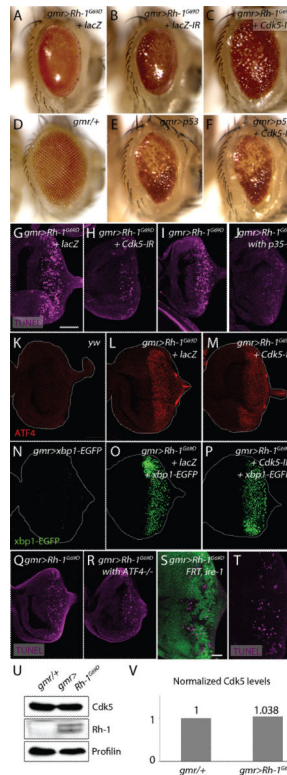


Figure 1. Cdk5 and its regulatory subunit p35 (Cdk5alpha) are required for Rh-1^{G69D}-induced apoptosis

(A–C) External adult eye phenotypes caused by overexpressing Rh-1^{G69D}, together with lacZ (A), or with inverted repeat (IR) transgenes to knockdown lacZ (B) and *cdk5* (C). Note a partial recovery of eye size upon *cdk5* knockdown. (D–F) *cdk5* knockdown does not affect the rough eye phenotype caused by p53-overexpression (E, F). (D) is a control fly eye with normal morphology. (G–J) Apoptosis in larval eye discs assessed through TUNEL (magenta). Misexpression of Rh-1^{G69D} led to massive apoptosis (G), which was suppressed by knocking down *cdk5* (H). Rh-1^{G69D}-triggered apoptosis (I), was also suppressed in a *p35* (*cdk5alpha*) $-/-$ background (J). (K–M) *cdk5* knockdown does not affect the degree of ATF4 protein induction (red) in response to Rh-1^{G69D} misexpression. Shown are; a control eye disc (genotype, *y, w*) (K), a disc misexpressing Rh-1^{G69D} together with a control lacZ transgene (L), or with a *cdk5-IR* transgene (M). (N–P) *cdk5* knockdown does not affect the degree of XBP1 pathway activation, as assessed through the XBP1-EGFP reporter (green). Shown are; a control eye disc expressing XBP1-EGFP alone (N), or together with Rh-1^{G69D} and lacZ (O), or with Rh-1^{G69D} and *cdk5-IR* (P). (Q, R) Rh-1^{G69D}-induced apoptosis in *ATF4 (crc)* $-/-$ discs. TUNEL (magenta) shows Rh-1^{G69D}-triggered apoptosis in *crc*⁺ (Q) and *crc*¹ $-/-$ discs (R). (S, T) Rh-1^{G69D}-induced apoptosis (magenta) in *ire1* $-/-$ clones (marked by the absence of green). The image is a magnified view of the region overexpressing Rh-1^{G69D}. TUNEL positive cells are found within the *ire1* $-/-$ clones. The scale bar in (G) represents 100 μ m for panels (G–R). (S, T) 20 μ m. Error bars show \pm SEM. Genotypes: *gmr-Gal4, UAS-Rh-1^{G69D}/UAS-lacZ;UAS-dicer2/+* (A, G, L), *gmr-Gal4, UAS-Rh-1^{G69D}/UAS-lacZ-IR;UAS-dicer2/+* (B), *gmr-Gal4, UAS-Rh-1^{G69D}/UAS-cdk5-IR;UAS-dicer2/+* (C, H, M), *gmr-Gal4/+* (D), *gmr-Gal4,UAS-p53/+;UAS-dicer-2/+* (E), *gmr-Gal4,*

UAS-p53/UAS-cdk5-IR;UAS-dicer2/+ (*F*), gmr-Gal4/UAS-Rh-1^{G69D};+/+ (*I*), gmr-Gal4, Df(p35)^{C2};UAS-Rh-1^{G69D}, Df(p35)^{20C} (*J*), y,w (*K*), gmr-Gal4/+;UAS-xbp1-EGFP/+ (*N*), gmr-Gal4, UAS-Rh-1^{G69D}/UAS-lacZ;UAS-dicer2/UAS-xbp1-EGFP (*O*), gmr-Gal4, UAS-Rh-1^{G69D}/UAS-cdk5-IR;UAS-dicer2/UAS-xbp1-EGFP (*P*), gmr-Gal4/UAS-Rh-1^{G69D} (*Q*), gmr-Gal4, crc¹/crc¹, UAS-Rh-1^{G69D} (*R*), gmr-Gal4, ey-flp/+; UAS-Rh-1^{G69D}/+; FRT82, ire1^{f02170}/FRT82, ubi-GFP (*S*, *T*).

Author Manuscript

Author Manuscript

Author Manuscript

Author Manuscript

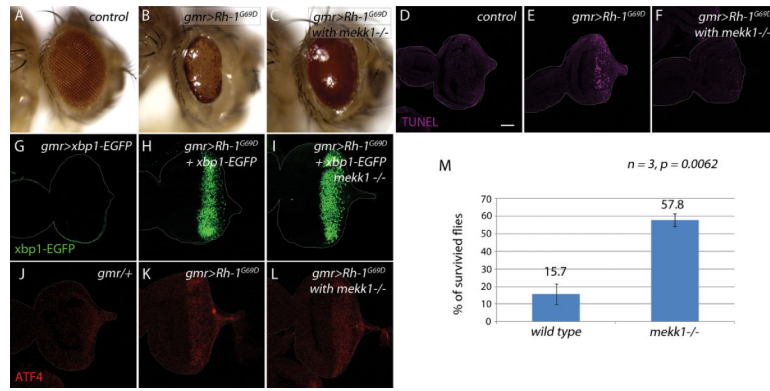


Figure 2. *Drosophila* Mekk1 is required for Rh-1^{G69D} to trigger apoptosis

(A–C) External adult eyes. A control adult eye with wild type morphology is shown in (A). The degree of eye ablation as a result of Rh-1^{G69D} misexpression (B), was suppressed in a *mekk1^{ur-36} -/-* background (C). (D–F) Apoptosis in eye discs as assessed through TUNEL labeling (magenta). A control eye disc shows little apoptosis (D). Massive apoptosis caused by Rh-1^{G69D} misexpression (E), is strongly suppressed in a *mekk1^{ur-36} -/-* background (F). (G–I) The degree of ER-stress as estimated through the *xbp1-EGFP* reporter (green). Control eye discs show little signs of ER stress (G). The degree of *xbp1-EGFP* reporter activation by Rh-1^{G69D} misexpression is similar between *mekk1*⁺ discs (H) and *mekk1^{ur-36} -/-* discs (I). (J–L) anti-ATF4 antibody labeling (red) is not affected by *mekk1*. A control disc (J). ATF4 is induced in Rh-1^{G69D} expressing discs (K), and is not affected in a *mekk1 -/-* background (L). (M) *mekk1* mutants are more resistant to Tunicamycin (Tm) feeding. 4–5 days old male flies (20–25 flies in each vial) were allowed to feed for 7 days with standard cornmeal medium supplemented with 5 ug/ml Tm. The percentage indicates the number of flies survived from feeding with Tm ($n = 3, p = 0.0062$). The scale bar in (D) represents 100 μm for all panels. Error bars show \pm SEM. Genotypes: *gmr-Gal4/UAS-Rh-1^{G69D};+/+* (B, E, K), *gmr-Gal4/UAS-Rh-1^{G69D};mekk1^{ur-36}/mekk1^{ur-36}* (C, F, L), y (D), *gmr-Gal4/UAS-*xbp1-EGFP*;+/+* (G), *gmr-Gal4, UAS-Rh-1^{G69D}/UAS-*xbp1-EGFP*;+/+* (H), *gmr-Gal4, UAS-Rh-1^{G69D}/UAS-*xbp1-EGFP*;mekk1^{ur-36}/mekk1^{ur-36}* (I), *gmr-Gal4/+* (J).

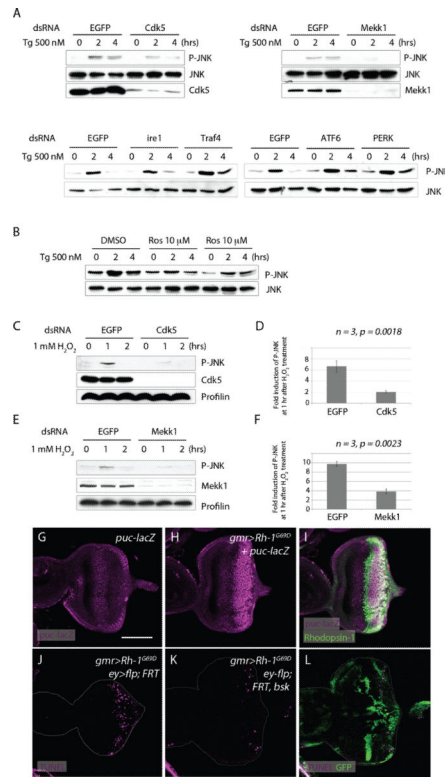


Figure 3. Mekk1 and Cdk5 mediate JNK signaling activation in response to stress

(A) Thapsigargin (Tg) treatment induces JNK phosphorylation dependent on *cdk5* and *mekk1*. Cells pre-treated with dsRNA against EGFP (negative control) show anti-phospho JNK blots after 2 hours of Tg treatment. Pre-treatment of dsRNAs against *cdk5* or *mekk1* reduces JNK phosphorylation, while dsRNAs against *ire1*, *traf4*, *atf6* and *perk* do not have obvious effects. (B) The role of *cdk5* was further assessed by pre-treating cells with the Cdk5 inhibitor, Roscovitine (Lanes 4–9). Control cells were pre-treated with DMSO (Lanes 1–3). (C–F) *cdk5* and *mekk1* mediates JNK phosphorylation in response to H_2O_2 treatment. (C) H_2O_2 induced JNK phosphorylation analyzed in cells pretreated with dsRNAs either against EGFP (Lanes 1–3) or *cdk5* dsRNA (Lanes 4–6). Anti-Cdk5 blot (middle panel) shows the degree of Cdk5 knockdown by RNAi. (D) Quantification of anti-phospho JNK bands after 1 hour of H_2O_2 treatment, with either a control dsRNA against EGFP or against *cdk5*, shows a statistically significant change ($n=3$, $p=0.0018$). (E) H_2O_2 induced JNK phosphorylation in cells pre-treated with dsRNAs against either EGFP (lanes 1–3) or *mekk1* (4–6). Anti-Mekk1 blot (middle panel) shows the degree of Mekk1 knockdown by RNAi. (F) Quantification of phospho JNK bands after 1 hour of H_2O_2 , from cells pretreated with dsRNA against either EGFP or *mekk1*, shows a statistically significant difference ($n=3$, $p=0.0023$). (G–I) Rh-1^{G69D} expression (green) activates JNK signaling in eye imaginal discs, as evidenced by the JNK reporter *puc-lacZ* (magenta) (H, I). (H) shows the anti-betaGal single channel of (I). (G) is a negative control without Rh-1^{G69D} expression. (J–L) The requirement of *bsk* (*Drosophila JNK*) in Rh-1^{G69D}-induced apoptosis. A control *bsk*+ disc expressing Rh-1^{G69D} shows many TUNEL positive cells (magenta) (J), which is suppressed in discs with *bsk* $-/-$ mosaic clones (K, L). *bsk* $-/-$ clones are marked by the absence of GFP (green). The scale bar in (G) represents 100 μ m. Genotypes: *gmr-Gal4/+;*

puc^{E69/+} (G), *gmr-Gal4,UAS-Rh-1^{G69D/+}*; *puc^{E69/+}* (H, I), *gmr-Gal4, ey-flp/+;UAS-Rh-1^{G69D/ubi-GFP, FRT40;+/+}* (J), *gmr-Gal4, ey-flp/+;bsk^{170B}, FRT40, UAS-Rh-1^{G69D/ubi-GFP, FRT40;+/+}* (K, L).

Author Manuscript

Author Manuscript

Author Manuscript

Author Manuscript

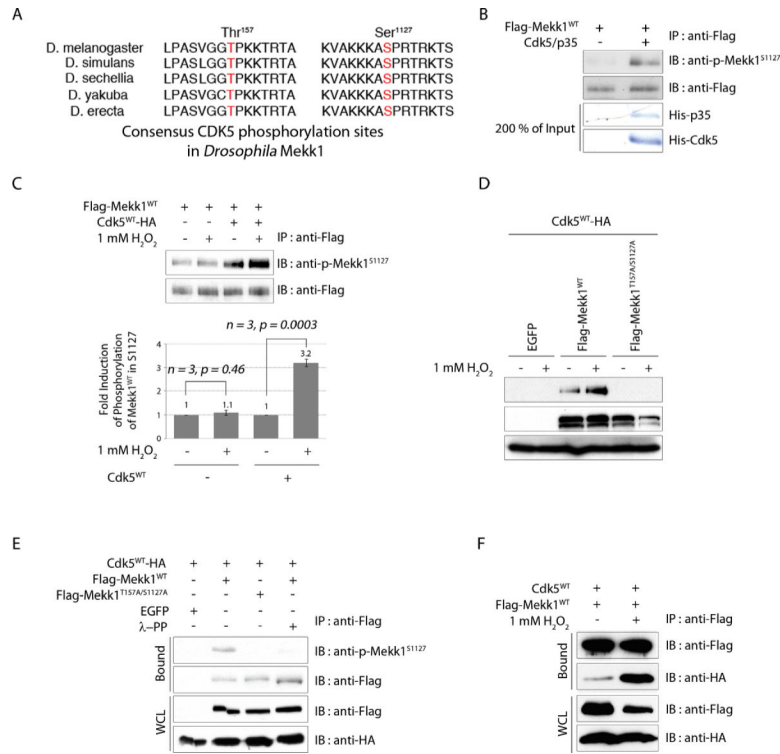


Figure 4. Cdk5 phosphorylates Meck1

(A) Conserved Cdk5 consensus phosphorylation sites within Meck1 of various *Drosophila* species. (B) Cdk5 phosphorylates Meck1^{WT} on the S1127 residue in vitro. Immunopurified Meck1 was incubated with recombinant Cdk5 and p35, and subsequently probed with an antibody against phospho S1127 residue of Meck1 (anti-p-Mek1^{S1127}). Anti-Flag blots show total Flag-tagged Meck1 levels (lower panel). (C) Phosphorylation at Meck1 in transfected cells. The Flag-tagged Meck1 was immunoprecipitated and probed with the anti-p-Mek1^{S1127} antibody. The average intensities of phospho Meck1 bands are shown in a graph underneath the blot. Only Cdk5 transfected cells show a statistically significant increase in Meck1 phosphorylation after H₂O₂ treatment ($n=3, p=0.0003$). (D) Validation of the Meck1 phosphorylation sites. HEK 293T cells were transfected with Cdk5, together with the indicated expression plasmids marked above the blot. Phospho-Mek1 bands do not appear when a mutant Meck1 plasmid lacking the putative phosphorylation sites are transfected (lanes 5, 6). Anti-Flag blots show Flag-tagged Meck1 levels (middle blot), while anti-HA bands show transfected Cdk5 levels (lower blot). (E) Meck1 phosphorylation bands disappear after phosphatase treatment (lane 4). Immunoprecipitated complex were either untreated or treated with λ -phosphatase (PP) prior to western blot analysis. (F) Coimmunoprecipitation of Cdk5 and Meck1. 293T cells were transfected with Flag-tagged Meck1^{WT}, together HA-tagged Cdk5^{WT}. The protein complexes were immunoprecipitated using anti-Flag antibody and analyzed by western blotting using anti-HA antibody. The interaction between Cdk5^{WT} and Meck1^{WT} was enhanced when cells were pretreated with H₂O₂ (lanes 2).

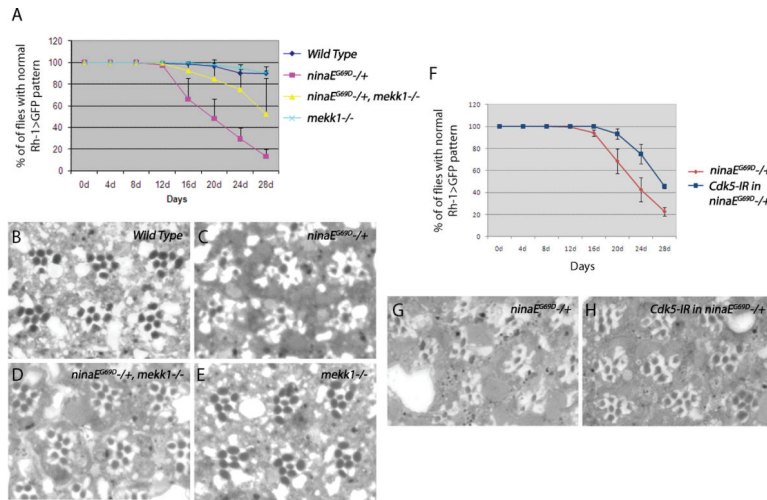


Figure 5. The course of late onset retinal degeneration of *ninaE^{G69D}/+* flies is delayed upon knockdown of Cdk5, or in the *mekk1^{ur-36}-/-* background

(A) Quantification of the degeneration process using the Rh1>GFP fluorescence. For each genotype, the percentage indicates the number of flies with intact ommatidial arrays as evidenced by Rh>GFP pattern, from an average of eight independent crosses. Loss of *mekk1* function delays the course of retinal degeneration of *ninaE^{G69D}/+* flies ($n = 8, p = 0.0062$). (B–E) Representative images of 20 day old adult eye tangential sections. Genotypes are as indicated in the panels. Wild type flies show clusters of seven rhabdomeres (stained as black circles) in a trapezoidal pattern within each ommatidia. While this pattern is disrupted in the *ninaE^{G69D}/+* retina, this degenerative phenotype is suppressed in *ninaE^{G69D}/+* with a *mekk1^{ur-36}-/-* background. (F) The knockdown of Cdk5 suppresses late onset retinal degeneration of *ninaE^{G69D}/+* flies ($n = 5, p = 0.0004$). (G, H) Representative images of 20 day old adult retina downregulating Cdk5 in the *ninaE^{G69D}/+* background.